ISSN 0965-545X, Polymer Science, Series A, 2021, Vol. 63, No. 6, pp. 793–799. © Pleiades Publishing, Ltd., 2021.
Russian Text © The Author(s), 2021, published in Vysokomolekulyarnye Soedineniya, Seriya A, 2021, Vol. 63, No. 6, pp. 422–429.

POLYMER BLENDS

Effect of Nanoscale Confinements on the Crystallization of Poly(ethylene oxide) in the Pores of Polyolefins Deformed by the Crazing Mechanism

A. Yu. Yarysheva[a,*], N. A. Sitnov[a], A. V. Bakirov[b,c], L. M. Yarysheva[a], M. S. Arzhakov[a], O. V. Arzhakova[a], and S. N. Chvalun[b, c]

[a] *Faculty of Chemistry, Moscow State University, Moscow, 119991 Russia*
[b] *National Research Center Kurchatov Institute, Moscow, 123098 Russia*
[c] *Enikolopov Institute of Synthetic Polymer Materials, Russian Academy of Sciences, Moscow, 117393 Russia*
**e-mail: alyonusha@gmail.com*

Received April 29, 2021; revised July 2, 2021; accepted July 16, 2021

Abstract—Polymer blends of polyolefins with poly(ethylene oxide) are obtained by the deformation of polypropylene and high-density polyethylene films in aqueous-ethanol PEO solutions by the crazing mechanism. The content of PEO with a molecular weight of 4×10^3 in the blends depends on the porosity of polyolefin matrices and grows with an increase in the degree of stretching of the films to 28% in HDPE–PEO blends and to 32% in PP–PEO blends. According to DSC studies, the crystallization of PEO is accompanied by decrease in the melting temperature by 4–6 K in the HDPE matrix and 6–7 K in the PP matrix and reduction in the degree of crystallinity by 24–49% in the HDPE matrix and 44–76% in the PP matrix compared with PEO crystallized in the "free" state. Using X-ray diffraction data, the sizes of crystallites of PEO with $M = 4 \times 10^3$ in the pores of polyolefins deformed by the crazing mechanism are first calculated, and it is shown that PEO macromolecules orient perpendicular to the axis of stretching of PP and HDPE matrices.

DOI: 10.1134/S0965545X21060146

INTRODUCTION

At present, systems in which the structuring of polymers is confined at the nanolevel are studied extensively. Among similar systems are thin polymer films or layers, polymers incorporated into nanoporous materials with different morphology of pores, miscible and immiscible polymer blends, block copolymers, nanofibers, nanotubes, nanocomposites, and many other systems, including those of biological origin [1–20]. The issues of polymer structuring under confined spatial conditions are considered for both amorphous glassy polymers and systems in which as if one of the components is capable of crystallization.

General features observed for polymers in a confined nanospace are primarily associated with a change in molecular mobility related to an increase in the ratio between the surface and bulk. As was shown for amorphous polymers, the glass transition temperature T_g in nanoscale dispersions, thin films, and surface layers decreases considerably compared with the corresponding value of the bulk polymer [2, 4, 9]. For crystallizable polymers, a change in T_g determines the lower boundary of the crystallization temperature, and the degree of supercooling (a difference between the temperature of crystallization of a polymer in the bulk and nanobulk) makes it possible to ascertain the mechanism of crystallization.

The effect of spatial confinements is firstly reflected in the nucleation process, because the critical size of the crystallization nucleus is usually several nanometers. As the volume of the polymer phase decreases, the mechanism of nucleation changes from heterogeneous typical of the bulk polymer to surface nucleation at the interfacial boundary and, in extreme cases, to homogeneous nucleation. The melting temperature also decreases with an increase in confinement, although to a lower extent. Bulk confinements also affect the kinetics of crystallization of polymers. In general, with an increase in the extent of confinement, the rate of crystallization slows down and the Avrami exponents decrease and can reach values equal to unity (or lower) [1, 6–8, 10, 11, 13, 20].

Note that, along with the general behavior of polymers under conditions of the confined space, for each of nanosystems (thin films, polymer blends, block copolymers, nanocomposites), the process of crystallization is influenced by its own characteristics and additional factors. A large number of fundamental studies on the effect of spatial confinements on the structuring of polymers was carried out for systems

based on porous matrices with the controlled size of pores, for example, track-etched membranes [21] and anodic alumina-based membranes containing regularly arranged cylindrical nanopores [1, 6, 8, 10–12, 14, 19].

In this study, polymers deformed by the crazing mechanism in physically active media and having the specific nanoporous structure were used as porous materials for introducing high molecular weight compounds and studying their structuring under spatial confinement conditions [8, 22–24]. Crazing provides a way not only to develop the porous structure in a polymer but also to obtain hybrid nanocomposites and polymer-polymer blends directly during the stretching of a polymer in active liquid media containing low molecular weight and high molecular weight compounds. The benefit of crazing is that change in the nature of physically active media and the conditions of polymer deformation (temperature and tensile strain) allows variation in the morphology and size of pores in the resulting porous structure, that is, the size of space hindering crystallization.

Poly(ethylene oxide) was chosen as introducing mixture component, which owing to its availability and narrow MMD is often used as a model polymer for studying the crystallization of polymers in systems, such as thin films, layered composites, and porous templates.

The goal of this study is to prepare polymer blends and to gain insight into the effect of nanoporous PP and HDPE matrices deformed by the crazing mechanism on the crystallization of PEO.

EXPERIMENTAL

In this study, Moplen PP films with a thickness of 90 μm, Stamylan HDPE films with a thickness of 25 μm, and semidilute 20 wt % aqueous-ethanol (85% ethanol) solution of PEO (Sigma–Aldrich) with $M_w = 4 \times 10^3$ were used. Films with a gage size of 20 × 40 mm were stretched in PEO solution at a rate of 5 mm/min using an Instron-1122 dynamometer. Afterwards, the samples were wiped and dried in vacuum. The volume porosity of the polymer during stretching was determined from a change in the geometric sizes of the samples: $W = (V_t - V_0)/V_t$, where V_t is the volume of the sample after stretching and V_0 is the initial volume of the sample. The content of PEO in the blends was assessed by the weight method $\Delta m/m_t = (m_t - m_0)/m_t \times 100\%$, where m_0 is the initial film weight and m_t is the blend weight. The average measurement error was ± 2%. The theoretical content of PEO in the blends was calculated under assumption that the total pore volume ($W = \Delta V/V_t$) is occupied by solution of 20% concentration C: $\Delta m/m_t$ (theory) = $CW_t/[(1 - W_t)\rho + CW_t] \times 100\%$, where ρ is the density of 0.95 g cm^{-3} for HDPE and 0.91 g cm^{-3} for PP.

The structure of the deformed polymers was studied by atomic force microscopy on a Solver BIO Olympus microscope (MDT Nanotekhnologiya, Russia). Scanning was carried out in the contact mode. The AFM images were treated using the FemtoScan Online program. The degree of crystallinity of PEO was calculated by the formula: $\chi = \Delta H/\Delta H_{100\%} \times 100\%$, where $\Delta H_{100\%} = 196.8$ J g^{-1} is the heat of fusion of the ideal PEO crystal. The value of ΔH was calculated from the DSC data (TA 4000 thermal analyzer, Mettler), the weight of the samples was 1–2 mg, and the rate of heating was 10 K/min.

Wide-angle X-ray diffraction analysis of the polymer blends was performed on the DIKSI beamline of the Kurchatov synchrotron. The radiation source was a rotating magnet of 1.7 T generating a radiation of 7.65 keV (1.625 A) with a resolution of $(dE/E) \times 10^{-3}$ and a photon flux of 10^9. The beam size of the sample was 0.5 × 0.3 mm; diffraction patterns were measured using a Dectris Pilatus 1M detector.

RESULTS AND DISCUSSION

The deformation of semicrystalline polymers in physically active media by the intercrystallite (delocalized) crazing mechanism is accompanied by formation of a fibrillar-porous structure with the sizes of pores and fibrils in the nanoscale dimension range (Fig. 1). In accordance with [23–25], HDPE with the initial row structure and PP with the initial α-spherulite structure chosen for this study have common characteristic morphological signs of the development of deformation by the intercrystallite crazing mechanism: moving apart and fragmentation of lamellas, rearrangement of the lamellar structure into the fibrillar one and the subsequent orientation of fibrills in the stretching direction, and development of pores in the intercrystallite space the length and width of which increase with increasing tensile strain.

However, as is clear from Fig. 1, the deformation of the tested semicrystalline polymers has its own specific features related to their different initial supramolecular structure responsible for different morphology and parameters of the final porous matrices (Table 1). For example, upon deformation by the crazing mechanism to the same tensile strain (200%) for HDPE and PP shown in Fig. 1, the average values of the long period determined from the profiles of AFM sections as the distance between the tops of lamellas were 75 ± 36 nm (HDPE) and 45 ± 17 nm (PP) [23, 24]. This makes it possible to estimate the average length of pores with allowance made for a lamella thickness of ~60 nm for HDPE and 25 nm for PP. The width of pores measured by AFM as a distance between the tops of fibrills was determined for HDPE and PP at a tensile strain of 300% (for PP deformed to tensile strains of 100 and 200%, this parameter is close to the cantilever curvature radius; therefore, its unambigu-

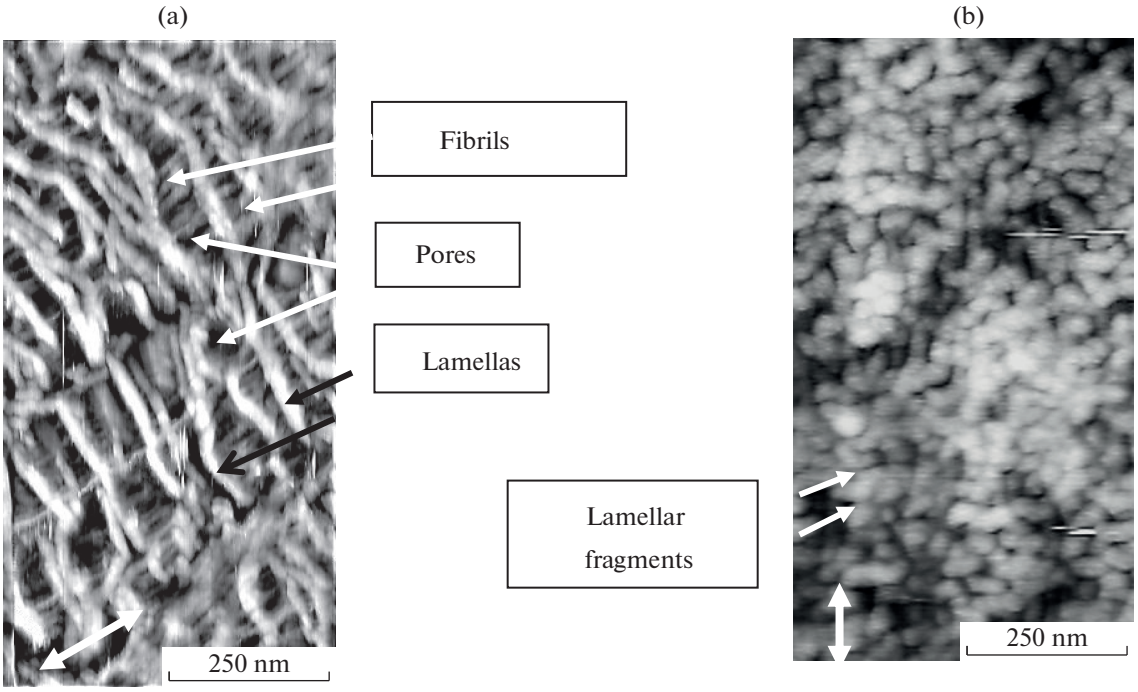

Fig. 1. AFM images of HDPE (a) and PP (b) deformed in physically active media by 200%. The arrows indicate the direction of stretching.

ous measurement is hardly possible). Note that, with an increase in the tensile strain, the average length of HDPE and PP pores and the width of HDPE pores increase (Table 1), but at the same tensile strain, the size of pores in HDPE is higher than the size of pores in PP. The revealed structural features at a similar chemical structure make matrices of polyolefins deformed by the crazing mechanism suitable model objects for studying the effect of spatial confinements on the structuring of crystallizable compounds introduced into nanopores.

The addition of PEO in the aqueous-ethanol solution functioning as a physically active medium insignificantly affects the process of deformation of PP and HDPE [26–28] and is accompanied by the penetration of PEO into the porous structure formed during crazing (Fig. 2a), as confirmed by an increase in the weight of the films (Fig. 2b) upon removal of the volatile liquid medium. With an increase in the tensile strain, the content of PEO grows in accordance with an increase in the porosity of the polymer matrix, and at all tensile strains, it is higher than the theoretical values calculated as described above under assumption of the full filling of pores with the PEO solution with a concentration of 20 wt %.

The dependence of the distribution coefficient (the ratio of polymer concentration in a pore to its concentration in solution) on the pore radius was studied in [29]. If there is no interaction between macromolecules and pore walls, the distribution coefficient is smaller than unity owing to the loss of entropy as a result of penetration of macromolecules into nanopores. However, the distribution coefficient in pores may increase sharply if there is interaction

Table 1. Pore size (long period *L*/pore width *D*) of deformed polyolefins and thermophysical properties of PEO in PP–PEO and HDPE–PEO blends

Tensile strain of PP and HDPE, %	*L*/*D*, nm		T_m of PEO, °C		Degree of crystallinity of PEO, %	
	HDPE [24]*	PP [23]*	HDPE–PEO	PP–PEO	HDPE–PEO	PP–PEO
100	55/19	36/–	56	55	45	18
200	75/20	47/–	58	56	58	38
300	100/33	55/23	58	56	70	50
PEO homopolymer			62		94	

*The average values are presented.

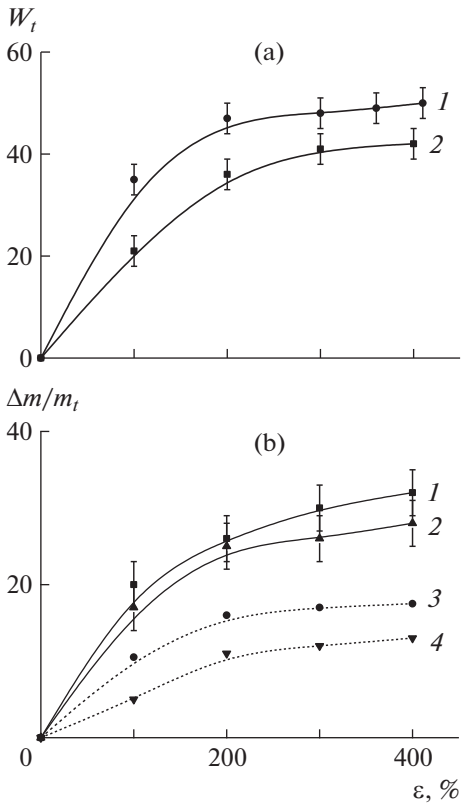

Fig. 2. (a) Dependence of porosity W on the tensile strain ε of (*1*) PP and (*2*) HDPE films in the aqueous-ethanol medium (85% ethanol), and (b) dependence of the content of PEO in (*1*) PP–PEO and (*2*) HDPE–PEO blends and the content of PEO in (*3*) PP–PEO and (*4*) HDPE–PEO blends calculated under assumption that the PP and HDPE pores are filled with the PEO solution with a concentration of 20%.

between macromolecules and pore walls [30–32]. It appears that the observed effect of PEO concentration is associated with its adsorption in the pores of deformed polymers which exhibit a good sorption behavior owing to their dispersion into nanoscale fibrillar aggregates and the formation of a highly developed surface (50–100 $m^2 g^{-1}$) during the process of crazing [22–24].

According to the thermophysical study, the thermograms of the obtained blends show two separate endothermic peaks corresponding to melting of the polymer matrix and PEO, which is evidence for phase separation of the components. The melting temperatures of HDPE and PP in the blends remain unchanged compared with the initial polymers. However, as opposed to the "free" crystallization in bulk, the crystallization of PEO in PP and HDPE nanopores entails a change in the fundamental characteristics of PEO and is accompanied by decrease in the degree of crystallinity and the melting temperature of PEO in the blends compared with PEO crystallized in the bulk (Table 1, Fig. 3).

Depending on the tensile strain, the degree of crystallinity of PEO decreases by 24–49% in HDPE-based blends and by 44–76% in PP-based blends in which the sizes of pores are much smaller than those in HDPE films. The melting temperature of PEO decreases by 4–6 K in the HDPE blends and 6–7 K in the PP blends.

The data obtained are consistent with the results of studying the crystallization of polymers under confined conditions where the growth of lamellas as if in one direction is limited to nanometer sizes: in thin films on the surface of substrates or thin layers of coextruded films, block copolymers and polymer blends containing PEO as a separate phase, PEO solutions or melts containing highly dispersed particles, and nanoporous materials [1–20]. As was shown in the cited studies, under conditions of spatial confinements, the degree of crystallinity and the melting temperature of PEO decrease. The smaller the confinement size (the pore diameter) down to the full loss of crystallizability of the polymer, the more distinct the reduction in the degree of crystallinity [1, 3, 6–8, 33, 34]. During the crystallization of polymers in the confined space, the process of nucleation prevails over the process of crystal growth, which leads to a decrease in the sizes of crystallites and an increase in their interfacial surface area [35]. As a result, the melting of these crystallites occurs at a lower temperature. It is evident that the same reasons are behind reduction in the melting temperature of PEO in PP–PEO and HDPE–PEO blends. Decrease in the degree of crystallinity can apparently be explained by the fact that a part of PEO in the nanoporous structure of PP and HDPE occurs under conditions where PEO is incapable of crystallization because of spatial confinements. In addition, the adsorption of PEO on the well-developed surface of the polymers deformed by the crazing mechanism may slow down the mobility of macromolecules in the surface layer and thus hinder their crystallization [34].

As is clear from Table 1, the higher the tensile strain during crazing, the larger the size of pores developed in the polymer matrix. A change in the sizes of PP and HDPE nanopores, which function here as a space confining the crystallization of PEO, affects the structure of PEO in the resulting blends. In fact, an increase in the tensile strain of HDPE and PP leads to a rise in the degree of crystallinity of PEO in the blends, although they never reach the values of PEO crystallized in the bulk (Table 1).

A difference in the melting temperatures of PEO in the blends compared with the initial homopolymer also decreases with increasing tensile strain of the films (Fig. 3). For example, for the PP–PEO blends obtained by the deformation of PP in a PEO solution to a tensile strain of 100%, the degree of crystallinity of PEO is as low as 18% and the melting temperature drops by seven degrees compared with the homopoly-

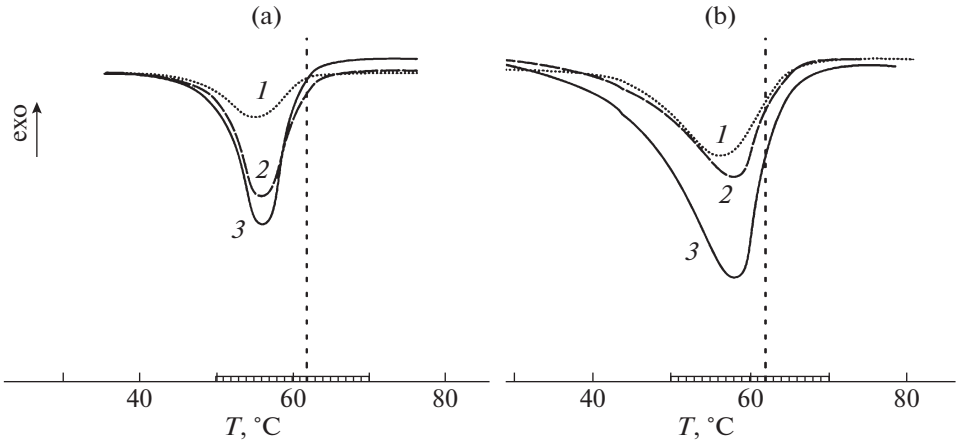

Fig. 3. Melting thermograms of PEO with $M = 4 \times 10^3$ in (a) PP–PEO and (b) HDPE–PEO blends depending on the tensile strain of polymers by (*1*) 100, (*2*) 200, and (*3*) 300%. The dashed line denotes the melting temperature of the bulk PEO.

mer. For the blend obtained by the deformation of PP in the same PEO solution to a tensile strain of 300%, the degree of crystallinity of PEO increases to 50% and the melting temperature is six degrees lower compared with the homopolymer. Similar effects are observed for the HDPE–PEO blends (Table 1; Fig. 3).

A comparison of the thermophysical properties of the blends based on PP and HDPE and an analysis of AFM images (Fig. 1) allow us to assume that a more pronounced decrease in the melting temperature and degree of crystallinity of PEO in the PP–PEO blends compared with the HDPE-based blends can be attributed to the fact that, at the same tensile strains, the sizes of PP pores, as shown above, are 2–3 times smaller than the sizes of HDPE pores. Thus, the process of crystallization of PEO is indeed controlled by spatial confinements of the nanoporous polymer matrix.

The wide-angle X-ray diffraction of polymer-polymer blends obtained by the deformation of polyolefins in PEO solutions to a tensile strain of 200% made it possible to estimate the sizes of the coherent scattering region for PEO crystallites. It was found to be 15 nm (in the equatorial direction) and 21 nm (in the meridional direction) in the HDPE matrix and 10 nm (in the equatorial direction) and 18 nm (in the meridional direction) in the PP matrix.

An analysis of X-ray scattering pictures of PP–PEO and HDPE–PEO samples made it possible to determine the orientation of PEO macromolecules relative to the stretching direction (Fig. 4). On the scattering curves, along with the reflections of HDPE (110, 200) and PP (110, 040, 130, 111, and 131/041), there are PEO reflections (120) and overlapping reflections (112/004) corresponding to interplanar distances of 4.63 and 3.86/3.97 Å typical of the monoclinic structure [36]. It is seen that, in both the PP and HDPE matrices, the PEO peak (120) in the meridional direction is much higher than that in the equatorial direction (Figs. 4a, 4b). The azimuthal distributions of the intensity of PEO reflection (120) in the PP–PEO and HDPE–PEO blends showed the presence of maxima at an angle of 90° to the equator (on the meridian) (Fig. 4c). Local maxima at 0° and 180° azimuthal angles appear owing to the superposition of reflections of PEO (120) and PP (130). Thus, in the PP–PEO and HDPE–PEO blends, the axes of PEO macromolecules are perpendicular to the axis of stretching or slightly deviate from this direction. This makes it possible to state that PEO macromolecules are oriented predominantly in the direction perpendicular to the axis of stretching of polyolefins or state the planar orientation of PEO lamellas relative to fibrills, as schematically shown in Fig. 4d.

The appearance of orientation of PEO macromolecules during crystallization in nanopores, that is, in the confined space, is associated with the crystallization features of macromolecular compounds [3, 6–8, 10–16, 19, 37, 38]. The free surface energy of a face formed by the folds of macromolecules is much higher than the free energy of side surfaces: the planar orientation of lamellas relative to the substrate should prevail. However, depending on the nature of interaction between a crystallizable polymer and a substrate, the geometry of the confined space, and the conditions of crystallization, different orientations of lamellas are possible. For example, the authors of [28] observed the parallel orientation of PEO lamellas with a molecular weight of 20×10^3 relative to PP and HDPE fibrills.

Evidently, the geometry and size of pores as a confinement factor and the interaction of the crystallizable polymer with the substrate surface influence the processes of nucleation and growth of crystals. In the PP–PEO and HDPE–PEO blends, the pore space is infiltrated with nanofibrils formed upon deformation of polyolefins by the crazing mechanism, and the nucleation of PEO apparently occurs on their surface.

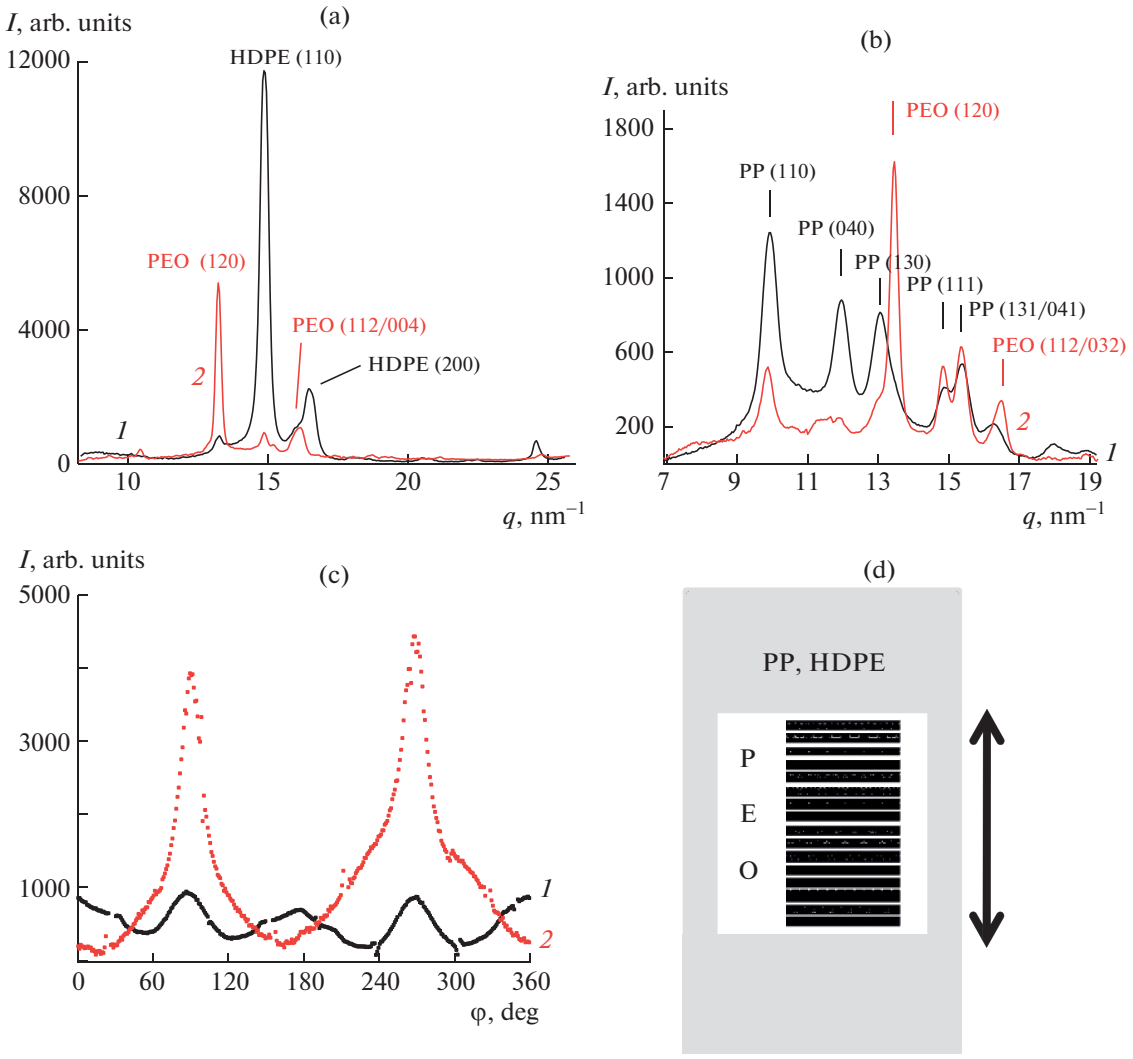

Fig. 4. WAXS curves in (*1*) equatorial and (*2*) meridional directions for (a) HDPE–PEO and (b) PP–PEO blends; (c) the azimuthal distribution of the intensity of PEO reflection (120) in (*1*) PP and (*2*) HDPE; and (d) schematic orientation of long axes of PEO macromolecules with $M = 4 \times 10^3$ in the pores of polyolefins deformed by the crazing mechanism.

Nucleation on the surface of nanofibrils may also be promoted by the adsorption of PEO preceding crystallization (Fig. 2b). At a contour length of 253.2 Å [39] of PEO macromolecules with a molecular weight of 4×10^3 and crystallite sizes of 100–210 Å, PEO can crystallize to form no more than one–two folds. It can be assumed that during adsorption a part of PEO macromolecules remains bound to the surface of PP and HDPE fibrils, and the remaining part is too small to form folds and PEO crystallizes with straightened chains perpendicular to the axis of stretching of PP and HDPE.

CONCLUSIONS

Thus, it is shown that PEO crystallizes in nanopores with HDPE and PP deformed by the crazing mechanisms and crystallization is accompanied by reduction in the melting temperature and the degree of crystallinity compared with the "freely" crystallized PEO. Reduction in the basic thermophysical characteristics of PEO is associated with spatial confinements arising during the process of crystallization and depends on the pore size of polymer matrices, which is determined by the tensile strain and the initial morphology of polyolefins, the row structure of HDPE and the spherulite structure of PP. The process of crystallization of PEO in nanopores is accompanied by the orientation of macromolecules perpendicular to the direction of stretching and, accordingly, the planar orientation of PEO lamellas. Thus, the pore sizes of HDPE and PP deformed by the crazing mechanism control the structuring of the infiltrated PEO. The observed effect may be of practical interest for producing PEO-based materials with a decreased degree of

crystallinity used as gas separation membranes or solid polyelectrolytes.

FUNDING

This work was supported by the Ministry of Science and Higher Education of the Russian Federation (agreement no. 075-15-2020-794).

REFERENCES

1. L. Sangroniz, B. Wang, Y. Su, G. Liu, D. Cavallo, D. Wang, and A. J. Muller, Prog. Polym. Sci. **115**, 101376 (2021).
2. M. Arutkin, E. Raphaël, J. Forrest, and T. Salez, Phys. Rev. J. **101**, 032122 (2020).
3. C. Yu, Q. Xie, Y. Bao, G. Shan, and P. Pan, Crystals **7**, 147 (2017).
4. D. Cangialosi, A. Alegría, and J. Colmenero, Prog. Polym. Sci. **54–55**, 128 (2016).
5. C. Mijangos, R. Hernández, and J. Martín, Prog. Polym. Sci. **54–55**, 148 (2016).
6. R. M. Michell and A. J. Müller, Prog. Polym. Sci. **54–55**, 183 (2016).
7. R. E. Prud'homme, Prog. Polym. Sci. **54–55**, 214 (2016).
8. A. L. Volynskii, A. Yu. Yarysheva, E. G. Rukhlya, L. M. Yarysheva, and N. F. Bakeev, Polym. Sci., Ser. A **57**, 515 (2015).
9. M. D. Ediger and J. A. Forrest, Macromolecules **47**, 471 (2014).
10. R. M. Michell, I. Blaszczyk-Lezak, C. Mijangos, and A. J. Muller, J. Polym. Sci., Part B: Polym. Phys. **52**, 1179 (2014).
11. R. M. Michell, I. Blaszczyk-Lezak, C. Mijangos, and A. J. Müller, Polymer **54**, 4059 (2013).
12. M. C. Lin, B. Nandan, and H.-L. Chen, Soft Matter **8**, 3306 (2012).
13. J. M. Carr, D. S. Langhe, M. T. Ponting, A. Hiltner, and E. Baer, J. Mater. Res. **27**, 1326 (2012).
14. H. Wu, Z. Su, and A. Takahara, Soft Matt **8**, 3180 (2012).
15. J. Martín, J. Maiz, J. Sacristan, and C. Mijangos, Polymer **53**, 1149 (2012).
16. H. Li and S. Yan, Macromolecules **44**, 417 (2011).
17. R. Chen and D. Huang, Front. Chem. China **6**, 332 (2011).
18. K. Chrissopoulou, K. S. Andrikopoulos, S. Fotiadou, S. Bollas, C. Karageorgaki, D. Christofilos, G. A. Voyiatzis, and S. H. Anastasiadis, Macromolecules **44**, 9710 (2011).
19. *Adsorption and Phase Behaviour in Nanochannels and Nanotubes,* Ed. by L. J. Dunne and G. Manos (Springer Science+Business Media B. V., Dordrecht; Heidelberg; London; New York, 2010).
20. Y.-X. Liu and E.-Q. Chen, Coord. Chem. Rev. **254**, 1011 (2010).
21. A.-K. Grefe, B. Kuttich, L. Stühn, R. Stark, and B. Stühn, Soft Matt **15**, 3149 (2019).
22. A. Yu. Yarysheva, O. V. Arzhakova, L. M. Yarysheva, and A. L. Volynskii, Polymer **158**, 243 (2018).
23. A. Yu. Yarysheva, D. V. Bagrov, A. V. Bakirov, L. M. Yarysheva, S. N. Chvalun, and A. L. Volynskii, Eur. Polym. J. **100**, 233 (2018).
24. A. Yu. Yarysheva, E. G. Rukhlya, L. M. Yarysheva, D. V. Bagrov, A. L. Volynskii, and N. F. Bakeev, Eur. Polym. J. **66**, 458 (2015).
25. A. Yarysheva, E. Rukhlya, T. Grokhovskaya, A. Dolgova, and O. V. Arzhakova, J. Appl. Polym. Sci. **136**, 48567 (2019).
26. A. Y. Yarysheva, A. A. Dolgova, L. M. Yarysheva, and O. V. Arzhakova, Mendeleev Commun. **30**, 507 (2020).
27. A. Y. Yarysheva, D. V. Bagrov, L. M. Yarysheva, A. L. Volynskii, and N. F. Bakeev, Polym. Sci., Ser. A **54**, 779 (2012).
28. A. Y. Yarysheva, D. V. Bagrov, A. V. Bakirov, B. N. Tarasevich, T. E. Grohovskaya, L. M. Yarysheva, S. N. Chvalun, and A. L. Volynskii, Macromolecules **50**, 2881 (2017).
29. E. F. Casassa and Y. Tagami, Macromolecules **2**, 14 (1969).
30. Y. Caspi, D. Zbaida, H. Cohen, and M. Elbaum, Macromolecules **42**, 760 (2009).
31. H. Grull, R. Shaulitch, and R. Yerushalmi-Rozen, Macromolecules **34**, 8315 (2001).
32. I. Teraoka, K. H. Langley, and F. E. Karasz, Macromolecules **26**, 287 (1993).
33. K. Shin, E. Woo, Y. G. Jeong, C. Kim, J. Huh, and K.-W. Kim, Macromolecules **40**, 6617 (2007).
34. W. Thitisomboon, Q. Gu, Lu-Tao. Weng, and P. Gao, Polymer **217**, 123449 (2021).
35. J. Maiz, J. Martin, and C. Mijangos, Langmuir **28**, 12296 (2012).
36. Y. Takahashi and H. Tadokoro, Macromolecules **6**, 672 (1973).
37. Y. Guan, G. M. Liu, P. Y. Gao, L. Li, G. Q. Ding, and D. J. Wang, ACS Macro Lett. **2**, 181 (2013).
38. X. Su Li X. Zhang, A. J. Müller, D. Wang, and G. Liu, Macromolecules **51**, 9484 (2018).
39. Yu. K. Godovskii, G. L. Slonimskii, and N. M. Garbar, Vysokomol. Soedin., Ser. A **15**, 813 (1973).

Translated by T. Soboleva